Delivery of loaded MR1 monomer results in efficient ligand exchange to host MR1 and subsequent MR1T cell activation

[Corinna A. Kulicke[1], Gwendolyn M. Swarbrick[2]], Nicole A. Ladd[3], Meghan Cansler[2], Megan Null[2], Aneta Worley[1], Chance Lemon[1], Tania Ahmed[2], Joshua Bennett[2], Taylor N. Lust[1], Chelsea M. Heisler[1], Megan E. Huber[5], Jason R. Krawic[6], Laurisa M. Ankley[7], Savannah K. McBride[5], Fikadu G. Tafesse[5], Andrew J. Olive[7], William H. Hildebrand[6], Deborah A. Lewinsohn[2], Erin J. Adams[3], David M. Lewinsohn[1,4], Melanie J. Harriff*[1,4, 5]

Affiliations

[1]Division of Pulmonary, Allergy, and Critical Care Medicine, Oregon Health & Science University, Portland, OR 97239, USA

[2]Division of Infectious Diseases, Department of Pediatrics, Oregon Health & Science University, Portland, OR 97239, USA

[3]Department of Biochemistry and Molecular Biology, University of Chicago, Chicago, IL 60637, USA

[4]VA Portland Health Care System, Portland, OR 97239, USA

[5]Department of Molecular Microbiology and Immunology, Oregon Health & Science University, Portland, OR 97239, USA

[6]Department of Microbiology and Immunology, University of Oklahoma Health Sciences Center, Oklahoma City, OK 73104, USA

[7]Department of Microbiology and Molecular Genetics, College of Osteopathic Medicine, Michigan State University, East Lansing, MI 48824 , USA

* corresponding author: harriffm@ohsu.edu

Keywords

MAIT cells, MAIT cell ligands, MR1-restricted T cells, antigen presentation, cellular immune response, mucosal immunology, T-cell

Abstract

MR1-restricted T cells have been implicated in microbial infections, sterile inflammation, wound healing and cancer. Similar to other antigen presentation molecules, evidence supports multiple, complementary MR1 antigen presentation pathways. To investigate ligand exchange pathways for MR1, we used MR1 monomers and tetramers loaded with 5-(2-oxopropylideneamino)-6-d-ribitylaminouracil (5-OP-RU) to deliver the antigen. Using MR1-deficient cells reconstituted with wild-type MR1 or MR1 molecules that cannot bind 5-OP-RU, we show that presentation of monomer-delivered 5-OP-RU is dependent on cellular MR1 and requires the transfer of ligand from the soluble molecule onto MR1 expressed by the antigen presenting cell. This new mode of antigen delivery strengthens the evidence for post-ER ligand exchange pathways for MR1, which could represent an important avenue by which MR1 acquires antigens derived from endocytosed pathogens.

Introduction

MR1-restricted T (MR1T) cells respond to small molecule antigens presented in the context of MHC I-related protein 1 (MR1) and include mucosal associated invariant T (MAIT) cells, which express the canonical TRAV1-2 TCR alpha chain [1]. They are increasingly being recognized for their role in early responses to microbial infection, but also in non-infectious conditions including a variety of autoimmune disorders, wound healing and cancer (reviewed e.g. in [1, 2]). Despite the heightened interest in these donor-unrestricted T cells, the mechanisms governing the presentation of MR1T cell antigens remain incompletely defined.

Successful antigen presentation requires the antigen presenting molecule to leave the endoplasmic reticulum (ER), bind an antigen, and display the bound antigen at the cell surface for T cell receptor (TCR) recognition. How these three features are achieved mechanistically, what compartments they take place in, and in what sequence they occur differs substantially between antigen presentation pathways. For major histocompatibility complex (MHC) I/peptide complexes, antigen binding generally precedes, and is indeed required for, ER egress and followed by translocation to the cell surface (reviewed e.g. in [3]). MHC II and CD1 molecules, by

54 contrast, exit the ER bound to a surrogate ligand which is exchanged for antigenic ligand in the
55 endosomal compartment after internalization from the cell surface (reviewed e.g. in [4, 5]).

56 For MR1, an MHC I-like mode of antigen acquisition has been described in which more MR1
57 associates with β_2-microglobulin (β_2m) and acquires endoglycosidase H (EndoH) resistance upon
58 addition of ligand to the culture medium [6, 7]. In line with this, McWilliam, Mak, et al. have used
59 a fluorescently labelled MR1 antigen analogue to directly demonstrate loading of exogenous
60 ligand in the ER [7]. Studies have linked the mechanism for MR1 ER egress to the charge
61 neutralization of a lysine residue within the MR1 ligand binding groove, which has been
62 suggested to result in a conformational change conducive to ER egress [6, 7]. The most potent
63 MR1 ligand described to date, 5-OP-RU, forms a Schiff base with this lysine residue, resulting in
64 its neutralization [6, 8].

65 In addition, recent findings support the hypothesis that there are complementary, non-exclusive
66 presentation pathways for MR1, allowing the molecule to survey diverse intracellular
67 compartments [9-14]. Multiple lines of evidence suggest that ligand exchange can occur on pre-
68 loaded MR1 molecules and that this may take place in an endosomal compartment. Most
69 notably, releasing MR1 from the ER prior to antigen exposure by pre-incubation with the MR1
70 ligand 6-formylpterin (6-FP) enhances presentation of exogenous antigenic ligand to MR1T cells
71 [10]. In line with this, siRNA knock-down of proteins involved in the trafficking and recycling of
72 endosomal vesicles such as VAMP4, Rab6 [9], Stx4, Stx16, and VAMP2 [10] impairs MR1-
73 mediated antigen presentation. Based on these observations, we and others have proposed
74 ligand exchange in a post-ER compartment as a complementary mechanism for MR1 ligand
75 acquisition [6, 10, 11, 14]. In a mechanism akin to MHC II and CD1 molecules, we hypothesize
76 that MR1 molecules internalized from the cell surface can be re-loaded with microbial antigens
77 in the endosomal compartment and recycle to the cell surface to activate MR1T cells. Here we
78 investigate the mechanisms underlying MR1 ligand exchange using a novel delivery method for
79 MR1T cell antigens. We find that MR1 ligands are efficiently presented when delivered in the
80 context of soluble MR1 molecules. This presentation is dependent on host MR1 and involves the
81 transfer of antigen from the recombinant molecule onto MR1 protein expressed by the cell.

82 Building upon our previously described tetraSPOT assay [15], this new method, the exSPOT,
83 extends the tool box available to investigate MR1 biology and provides important insights into
84 the mechanisms of MR1-mediated antigen presentation.

85 Results

86 *MR1 ligands delivered to antigen presenting cells on soluble MR1 molecules are efficiently*
87 *recognized by an MR1T cell clone*

88 The MR1 ligand 5-OP-RU is inherently unstable in aqueous environments [8, 16], which
89 presumably includes the intracellular milieu. However, the formation of a covalent bond with the
90 lysine residue at position 43 of MR1 stabilizes the antigen [8]. We have successfully used such
91 MR1/5-OP-RU complexes in their tetramerized form in plate-bound assays to activate MR1T cells
92 [15]. Similarly, Priya and Brutkiewicz have used latex beads coated with MR1/5-OP-RU complexes
93 to expand and activate human MAIT cells [17]. While these studies used recombinant MR1
94 molecules immobilized on a scaffold, here we sought to improve the efficiency of ligand delivery
95 into physiologically relevant antigen presenting cells (APCs) using soluble MR1.

96 To test this system, we incubated human dendritic cells (DCs) with MR1 tetramers loaded with
97 the canonical ligand 5-OP-RU (exSPOT), or applied the same concentration of tetramer directly
98 to the ELISPOT plate prior to adding an MR1T cell clone (tetraSPOT). Intriguingly, the MR1T cells
99 readily produced IFN-γ in response to the DCs incubated with soluble MR1/5-OP-RU in a dose-
100 dependent manner (Figure 1a). As expected based on previous work [15], they also produced
101 IFN-γ in the tetraSPOT. A quantitative comparison between the two assays was not possible due
102 to unknown coating efficiency in the tetraSPOT. MR1T cells did not respond to the MR1/6-FP
103 tetramer in the tetraSPOT, but we observed MR1T responses to the MR1/6-FP tetramers
104 incubated with DCs at the highest concentrations (Figure 1a). Similar to the tetraSPOT [15], MR1T
105 cell activation by DCs incubated with soluble MR1 tetramers was dependent on MR1, as blocking
106 with the anti-MR1 antibody clone 26.5 markedly reduced the response (Figure 1b, EC_{50} of 0.95
107 pM *vs* 31.62 pM, $p<0.0001$). Thus, 5-OP-RU delivered in the context of soluble, recombinant MR1

108 is efficiently presented by DCs and activates a human MR1T cell clone in an MR1-dependent
109 manner.

110 As professional APCs, DCs are particularly well equipped for phagocytosis of particulates of
111 various sizes and cross-presentation [18]. To investigate whether such specific functionality was
112 required in the exSPOT, we incubated the monocytic cell line THP-1, a B cell line (LCL), or the
113 airway epithelial cell line BEAS-2B with MR1/5-OP-RU tetramers and quantified IFN-γ responses.
114 As with DCs, the MR1T cell clone produced IFN-γ in response to all of the tetramer-incubated cell
115 types (Figure 1c). However, DCs were nearly three orders of magnitude more efficient at
116 presenting the antigen compared to the other cell types (EC_{50} of 0.55 pM *vs* 142 – 265 pM,
117 $p<0.0001$).

118 *Ligand delivered in the context of MR1 monomer is presented more efficiently than free ligand*

119 Next, we compared the presentation of MR1/5-OP-RU tetramers and MR1/5-OP-RU monomers
120 to reduce the variability associated with tetramerization (e.g. biotinylation efficiency,
121 streptavidin binding, and ligand saturation). Using the MR1 monomer further circumvented
122 potential variability introduced by instability of the tetramer complex over time.

123 To our surprise, presentation of ligand from monomer-incubated DCs to MR1T cells was even
124 more efficient than presentation of ligand from tetramer-incubated DCs, when accounting for
125 valency (Figure 2a). Although the EC_{50} values of the complexes were comparable (Tetramer EC_{50}:
126 0.204 pM *vs* Monomer EC_{50}: 0.22 pM, $p=0.7517$), there was a marked difference in the estimated
127 EC_{50} for 5-OP-RU which takes into account that each tetramer carries up to four 5-OP-RU
128 molecules whereas each monomer carries one at most (Tetramer 5-OP-RU EC_{50}: 0.816 pM *vs*
129 Monomer 5-OP-RU EC_{50}: 0.22 pM, $p<0.0001$). Comparing monomer-delivered 5-OP-RU to free
130 ligand further revealed improved efficiency of the monomer over the unbound antigen (Figure
131 2a; Monomer EC_{50}: 0.22 pM *vs* Free EC_{50}: 4.97 pM, $p<0.0001$). Of note, these calculations assume
132 full occupancy of monomers and tetramers.

133 To further investigate the relative efficiency of loading free *vs* monomer-bound 5-OP-RU, we
134 wanted to specifically detect MR1 molecules bearing 5-OP-RU at the cell surface by flow

135 cytometry. To this end, we generated a TCR tetramer based on the TCR sequence of the same
136 previously characterized MR1T cell clone that was used in the functional assays (TRAV1-2^{+} clone
137 D426-G11 – see references [15, 19]). We confirmed that this reagent specifically stained MR1
138 molecules loaded with 5-OP-RU but not 6-FP (Supplementary Figure 1). When we incubated
139 BEAS-2B cells overexpressing GFP-tagged MR1 (BEAS-2B.MR1-GFP) with either MR1/5-OP-RU
140 monomer or free 5-OP-RU overnight and stained with the TCR tetramer to track the cell surface
141 translocation of MR1 bound to the antigen, almost 100-fold higher concentrations of free 5-OP-
142 RU were needed to reach cell surface levels comparable to monomer-delivered ligand (Figure
143 2b). Together, these results demonstrate that soluble, recombinant MR1 is an efficient
144 mechanism for delivery of MR1T cell antigens in a variety of cell lines *in vitro.*

145 *Presentation of MR1 ligands delivered on soluble MR1 molecules requires cellular MR1*

146 In principle, the MR1/5-OP-RU complex that interacts with the TCR in our assay could be either
147 endogenously expressed MR1 bound to 5-OP-RU from the monomer or the recombinant MR1/5-
148 OP-RU monomer itself. Thus, we tested whether endogenous MR1 was required. We incubated
149 WT BEAS-2B cells, MR1$^{-/-}$ BEAS-2B cells lacking all isoforms of MR1, and MR1$^{-/-}$ BEAS-2B cells
150 reconstituted with tetracycline-inducible MR1A [20, 21] with MR1/5-OP-RU monomer and used
151 them as APCs. As expected, we detected responses to WT BEAS-2B cells incubated with MR1/5-
152 OP-RU monomers (Figure 3a, left), but when these monomers were incubated with the MR1$^{-/-}$
153 BEAS-2B cell line, the response was completely abrogated (Figure 3a, middle). Reconstitution of
154 MR1 expression in MR1-deficient cells resulted in complete recovery of MR1T cell responses to
155 the monomer-delivered ligand (Figure 3a, right). These observations were confirmed in THP-1
156 cells (Figure 3b).

157 *Ligands are transferred from soluble MR1 molecules onto cellular MR1*

158 Having established that MR1 expression by the APC itself was required for presentation of
159 monomer-delivered ligand, we considered two possible scenarios: (1) dimerization or indirect
160 binding of the monomer to host MR1 at the cell surface and (2) uptake of the MR1/5-OP-RU
161 complex and transfer of the antigen from the monomer onto cellular MR1.

162 Since the MR1 molecules used to generate the ligand-loaded monomers and tetramers do not
163 contain a transmembrane domain [8], their presence on the cell surface and, hence, ability to
164 activate MR1T cells, would require lateral interactions with other membrane-bound proteins. Of
165 note, Lion and colleagues have demonstrated that a GFP-tagged version of the MR1B isoform
166 weakly associated with the MR1A isoform although that observation was considered a potential
167 technical artifact [22]. To directly investigate the presence of the monomer on the cell surface,
168 we incubated BEAS-2B.MR1-GFP cells with the biotinylated MR1/5-OP-RU monomer and stained
169 the cells with fluorophore-coupled streptavidin. We did not detect any signal from the
170 biotinylated monomer although our controls confirmed that we added sufficient monomer to
171 induce MR1 surface translocation and sufficient streptavidin to detect biotinylated molecules at
172 the cell surface (Figure 4a). Interestingly, we detected a small but notable shift in total MR1
173 surface levels after incubation with the monomer (Figure 4a, right). This suggests that enough 5-
174 OP-RU ligand is delivered to increase not just TCR-reactive, but overall MR1 surface levels.
175 Together, these data do not support MR1 dimer formation at the cell surface.

176 Since we could not find evidence for direct presentation by the monomer, we next tested the
177 hypothesis that the 5-OP-RU is transferred from the soluble MR1/5-OP-RU complex onto the MR1
178 expressed by the APC. First, we sought to establish whether actin-dependent internalization of
179 soluble MR1 molecules was required for the presentation of monomer-delivered 5-OP-RU. Thus,
180 we treated BEAS-2B.MR1-GFP cells with latrunculin B (LatB), a well-characterized inhibitor of
181 actin polymerization. Surface levels of 5-OP-RU-loaded MR1 were reduced in cells treated with
182 LatB as compared to the DMSO control (Figure 4b). Of note, LatB treatment also reduced surface
183 expression of TCR-reactive MR1 in response to free 5-OP-RU (Supplementary Figure 4a). Total
184 MR1 as measured by the GFP expression was not reduced by LatB treatment (Supplementary
185 Figure 4b). We concluded that an active actin cytoskeleton is required for presentation of the
186 monomer-derived ligand. This is consistent with previous results demonstrating a requirement
187 for actin for an efficient MR1 response to *Escherichia coli* (*E.coli*) [13, 23] and could indicate a
188 requirement for either internalization or intracellular trafficking.

189 Additional evidence that intracellular processing is required came from the observation that the
190 kinetics of presentation differ between monomer-delivered ligand compared to free 5-OP-RU.
191 Here, we incubated BEAS-2B.MR1-GFP cells with concentrations of MR1/5-OP-RU monomer (50
192 nM) and free 5-OP-RU (6.4 µM) that resulted in intermediate surface expression (Figure 2b) and
193 followed MR1 surface translocation over time. In agreement with McWilliam et al., who detected
194 surface expression of 5-OP-RU-loaded MR1 after 2 h [6], we saw loaded MR1 as soon as 1 h after
195 addition of the free ligand (Figure 4c). By contrast, it took 6 h for the MR1 surface expression to
196 reach comparable levels after addition of the MR1/5-OP-RU monomer (Figure 4c). These kinetics
197 are consistent with a longer time needed for internalization, processing, ligand exchange, and
198 recycling of monomer-delivered ligand compared to free 5-OP-RU.

199 To directly investigate transfer onto cellular MR1, we tested whether the MR1 expressed by the
200 APC needed to be capable of presenting 5-OP-RU or whether its presence was sufficient. We
201 reconstituted the $MR1^{-/-}$ BEAS-2B cell line with a CRISPR-resistant version of MR1A that carried
202 the R9H mutation described by Howson et al. [24]. This mutation allows stable MR1 protein
203 expression and binding of 6-FP but renders the protein incapable of presenting 5-OP-RU ([24]
204 and Supplementary Figures 2 and 3). Indeed, reconstituting the MR1-deficient cells with this
205 mutant did not rescue the presentation of either monomer-delivered 5-OP-RU or *Mycobacterium*
206 *smegmatis (M. smegmatis)* supernatant (Figure 4d), further supporting the idea that it is the
207 cellular MR1 that presents the 5-OP-RU ligand.

208 *Ligand exchange occurs in post-ER compartments and does not require acidification*

209 Our data demonstrate the transfer of monomer-delivered 5-OP-RU onto MR1 expressed by the
210 APC but the mechanism of this exchange is unclear. Our lab has previously shown that pre-
211 incubation with the non-stimulatory ligand 6-FP can increase MR1-mediated antigen
212 presentation, presumably by increasing the pool of MR1 molecules available for ligand exchange
213 [10]. When we applied this concept to the monomer delivery assay, we found a similar effect:
214 releasing MR1 from the ER by pre-incubation with 6-FP decreased the EC_{50} for presentation of
215 monomer-delivered ligand from 1.027 pM to 0.1365 pM ($p<0.0001$; Figure 5a). Thus, MR1
216 molecules pre-loaded with a non-stimulating ligand appear to contribute to the activation of

217 MR1T cells after delivery of antigenic ligand on monomers, supporting the notion of ligand
218 exchange. In this context, it is worth noting that 6-FP concentrations multiple orders of
219 magnitude higher were required to inhibit 5-OP-RU presentation in a functional assay [25], which
220 suggests stronger binding of 5-OP-RU [6] and may help push the equilibrium towards binding of
221 the activating ligand.

222 To probe to what extent the monomer delivery could be extended to other antigen presentation
223 pathways and potentially gain mechanistic insights from any parallels, we repeated the assay
224 with peptide-loaded MHC I and II tetramers. We first used a fluorophore-conjugated HLA-
225 B*08:01/CFP10$_{3-11}$ tetramer to stain a CD8^{+} T cell clone restricted by this MHC I/peptide complex
226 (D480-F6 – see references [26] and [27]) for flow cytometry, confirming the T cell clone reacted
227 with the tetramer (Figure 5b). However, using the same tetramer to load autologous DCs in an
228 ELISPOT with the same T cell clone did not result in the production of IFN-γ in an APC-dependent
229 manner (Figure 5c). As expected, the T cells responded to DCs incubated with free peptide (Figure
230 5c). Next, we tested an HLA-DRB1*14:03/ESAT6$_{73-78}$ tetramer in combination with a T cell clone
231 that was specific to the antigen but restricted by a different MHC II allele (D481-D1, from an HLA-
232 DRB1*14:03 negative individual). As expected, this tetramer did not stain the T cell clone by flow
233 cytometry (Figure 5d). Nevertheless, feeding the non-matched tetramer to DCs autologous to the
234 same MHC II-restricted T cell clone elicited an IFN-γ response (Figure 5e). The only source of
235 matched MHC II molecules in this case are the DCs, further supporting a requirement for transfer
236 of the antigen from the soluble protein onto antigen presenting molecules expressed by the APC
237 itself. In line with this, the T cells did not respond when using HLA-mismatched DCs or the A549
238 cell line which express MHC II alleles different from Donor 481 ([28], Cellosaurus cell line A-549
239 (CVCL_0023) (expasy.org)) (Figure 5f). Thus, like with MR1, presentation of the MHC II antigen
240 delivered in the context of recombinant antigen presenting molecules requires transfer onto
241 proteins expressed by the APC.

242 Since soluble proteins could efficiently deliver peptide for MHC II presentation, we reasoned that
243 the MR1 loading in our assay was similar to the MHC II pathway, which involves exchange of a
244 surrogate ligand in an endosomal compartment (reviewed e.g. in [4]). To test whether MR1 ligand

245 transfer from the monomer could be mediated in an analogous fashion, we investigated the
246 effect of brefeldin A (BFA) on the presentation of monomer-delivered 5-OP-RU. BFA disrupts the
247 Golgi apparatus and effectively traps secretory proteins in the ER. Indeed, incubation with BFA
248 diminished surface translocation of 5-OP-RU-loaded MR1 in response to the MR1/5-OP-RU
249 monomer (Figure 5g, left). However, this experiment is unable to distinguish between two
250 different scenarios: 1) ligand exchange occurs in the ER and MR1 needs to subsequently traverse
251 the Golgi for surface presentation, or 2) MR1 needs to leave the ER to be available for exchange
252 in a post-ER compartment. To distinguish between these two hypotheses, we pre-incubated the
253 cells with 6-FP to induce ER egress of a pool of MR1 molecules before adding the BFA. Under
254 these conditions, BFA had a minimal effect on presentation of monomer-delivered ligand (Figure
255 5g, second from left). As expected, presentation of free 5-OP-RU was similarly impaired in the
256 presence of BFA and improved after pre-incubation with 6-FP (Supplementary Figure 5). It is
257 important to note that BFA treatment also reduced total MR1 levels as measured by GFP
258 expression (Figure 5g, right panels). These data clearly show that 5-OP-RU delivered on soluble,
259 recombinant MR1 molecules can be transferred to cellular MR1 in a post-ER compartment.

260 Exchange of exogenous ligand onto MHC II [4] and CD1 [5] molecules is potentiated by the low
261 pH in the endolysosomal compartment. Pertinently, endosomal acidification is required for
262 efficient presentation of *E.coli* by MR1 [13, 29] and McWilliam et al. have proposed that the Schiff
263 base that links 5-OP-RU to the MR1 ligand binding groove is labile under acidic conditions [6, 14].
264 Therefore, we investigated whether presentation of monomer-delivered ligand was dependent
265 on endosomal acidification using both a cell-free and a functional approach. First, we tested the
266 stability of the MR1/5-OP-RU and MR1/6-FP monomers under increasingly acidic conditions in
267 an ELISA. Fully folded, recombinant MR1 loaded with either 6-FP or 5-OP-RU was readily
268 detectable using both a conformation-dependent anti-MR1 antibody [30] and an anti-β_2m
269 antibody at neutral pH (Figure 6a). As expected, at neutral pH, a control MHC I/peptide complex
270 was detected by the anti-β_2m antibody but not by the anti-MR1 reagent and the recombinant γδ
271 TCR used as a control was detected by neither antibody. Since MR1 requires a ligand to efficiently
272 refold *in vitro* [8, 31], both read-outs specifically report on fully folded trimeric complexes.
273 Surprisingly, binding of neither the anti-MR1 nor the anti-β_2m antibody was affected by overnight

274 treatment of the plate-bound monomer with buffers of increasing acidity, covering the range of
275 those observed in the endomembrane compartments (pH 4.5-7.5). Acidic conditions, therefore,
276 did not destabilize the antibody-reactive conformation of MR1 in this assay. Hence, it appears
277 unlikely that loaded MR1 ligands are released simply by virtue of the acidic conditions in the
278 endosomal compartment.

279 To confirm these results in a cellular assay, we pre-incubated BEAS-2B WT cells with bafilomycin
280 before performing the exSPOT. Bafilomycin inhibits vacuolar ATPases [32] and diminishes the
281 presentation of an endosomal processing-dependent 5-A-RU pro-drug to MR1T cells [12].
282 Whereas the bafilomycin concentrations we used here reduced the MR1T cell response to this
283 pro-drug in a dose-dependent manner, presentation of the monomer-delivered 5-OP-RU was not
284 affected by the inhibitor (Figure 6b). Together, these data support a model in which the transfer
285 of 5-OP-RU delivered in the context of a soluble MR1 monomer onto the MR1 expressed by the
286 APC can displace pre-bound 6-FP and is independent of endosomal acidification.

287 Transfer of monomer-bound 5-OP-RU requires breaking a covalent bond. Since acidification was
288 not needed for ligand transfer (Figure 6b), we hypothesized that this process is catalyzed by an
289 exchange chaperone akin to HLA-DM for MHC II [4, 33]. TAPBPR, tapasin, and the adapter protein
290 AP2A1 have been shown to bind MR1 and modulate its antigen presentation [7, 34, 35]. However,
291 knock down (KD) of these candidate chaperones alone or together did not affect how efficiently
292 monomer-delivered 5-OP-RU was presented to our MR1T cell clone (Supplementary Figure 7).

293 To further characterize the compartment where ligand exchange in the exSPOT occurs, we
294 performed immunofluorescence microscopy. We observed AF647-labeled MR1/5-OP-RU
295 tetramer in compartments labeled with Rab5 (23.51%), an early endosome marker, or LAMP1
296 (33.1%), which localizes to late endosomes and lysosomes in these cells [36] (Figure 6c). These
297 observations support the hypothesis that ligand transfer occurs in post-ER compartments,
298 including the early and late endosome.

299 Vesicular trafficking between the cell surface and the endosomal compartments is mediated by
300 soluble N-ethylmaleimide-sensitive factor attachment protein receptors (SNAREs) [37]. The

301 SNARE syntaxin-4 (STX4) is required for exocytosis in various cellular contexts [38-41] including
302 the fusion of recycling endosomes to the plasma membrane in cytotoxic T cells [38] and post-
303 synaptic membranes on dendritic spines [39]. Our lab has previously shown that siRNA-mediated
304 knock down of STX4 reduces MR1-mediated antigen presentation of *M. smegmatis* supernatant
305 but not live *Mycobacterium tuberculosis* [10]. To investigate the involvement of this mediator of
306 vesicular trafficking in the exSPOT, we generated BEAS-2B cells deficient for STX-4 using
307 CRISPR/Cas9 technology. Consistent with previous results in the knock down system [10], STX-4
308 KO cells presented *M. smegmatis* supernatant less efficiently than their Cas9-expressing parent
309 cell line (Figure 6d, right, $p<0.0001$). Similarly, presentation of monomer-delivered antigen was
310 reduced in the absence of the SNARE (Figure 6d, left, $p=0.0032$). These results implicate STX4 in
311 the mechanism underlying the exSPOT and suggest that it may share mechanistic parallels with
312 presentation of microbial ligand.

313 Discussion

314 Distinct and complementary cellular pathways have been proposed for MR1 loading and
315 trafficking [11, 14, 42, 43]. While most research efforts have been focused on the ER pathway,
316 increasing evidence supports exchange in a post-ER compartment as a mechanism by which MR1
317 acquires antigenic ligand(s). For example, both Karamooz et al. and McWilliam et al. have shown
318 that MR1 molecules in cells pre-incubated with the MAIT cell antagonist 6-FP can present
319 activating MR1 ligands upon subsequent incubation with agonistic ligand [6, 10]. This exchange
320 requires internalization of the molecules and partially counters the ability of Brefeldin A (BFA) to
321 block surface expression of MR1/5-OP-RU complexes, indicating re-loading in a post-ER
322 compartment [6]. Indeed, pre-incubation with 6-FP enhances MR1-mediated presentation of
323 bacterial supernatant, presumably by increasing the pool of MR1 molecules available for re-
324 loading [10]. Using a fluorescence internalization probe (FIP), McWilliam et al. have directly
325 demonstrated recycling of a small proportion of MR1 molecules in C1R cells [6]. In our model of
326 mycobacterial infection of airway epithelial cells, this pathway contributes substantially to
327 presentation of antigen derived from intracellular infection [9, 10].

328 A recently developed pro-drug requires endosomal processing to release the 5-OP-RU precursor
329 5-A-RU [12]. Since the antigen is generated in endosomes in this scenario, it appears likely that
330 this compound is loaded onto MR1 in this compartment as opposed to trafficking to another
331 intracellular organelle, which would require it to cross multiple membranes. Interestingly, while
332 Ac-6-FP inhibits T cell activation after delivery of free 5-A-RU, it does not interfere with the
333 presentation of this pro-drug [12]. This is consistent with the earlier observation that 6-FP blocks
334 presentation of bacterial supernatant but not of intracellular infection [9]. Together, these results
335 suggest that there are distinct pools of MR1 in the ER and in a post-ER compartment [11, 12, 14,
336 43], that these compartments are differentially accessed by exogenous ligands, and/or that
337 conditions are more favorable for ligand exchange in the endosomal compartment than in the
338 ER. This notion is not without precedent as multiple, complementary pathways including both
339 direct loading in the ER and ligand exchange in the endosomal compartment have been shown
340 for MHC I (reviewed e.g. in [44]).

341 Of note, a synthetic MR1 ligand modified to be able to track its location by microscopy resides in
342 small vesicles also occupied by the micropinocytosis marker dextran [7]. This supports the idea
343 that both membrane-bound internalized MR1 and soluble MR1 ligands could occupy this
344 compartment at the same time, facilitating loading [14]. Furthermore, MR1-mediated antigen
345 presentation of *M. smegmatis* supernatant is reduced upon knock-down of endosomal trafficking
346 molecules [9, 10], further supporting involvement of this pathway in efficient loading of some
347 antigens.

348 In this study, we report a novel delivery method for MR1 ligands which allowed us to directly
349 demonstrate transfer of the MR1T cell-activating ligand 5-OP-RU from recombinant, soluble MR1
350 onto cellular MR1. Intriguingly, monomer-delivered antigen was presented more efficiently than
351 tetramer-delivered ligand. We speculate that the bulky structure of the tetramer may result in
352 steric hindrance of interactions with chaperones required for ligand transfer. The smaller, more
353 compact monomer, on the other hand, may be better suited to adopt the correct orientation.
354 Moreover, DCs were much more efficient at presenting the tetramer-derived ligand than other
355 cell lines tested. This could be due to their ability to cross-present internalized antigen, which

356 allows their MHC I molecules to sample diverse sources of antigen and may enable MR1 to do
357 likewise [18].

358 Monomer-delivered 5-OP-RU was also presented to MR1T cells more efficiently than free 5-OP-
359 RU. One explanation for this observation is that binding to the monomer protects the inherently
360 unstable antigenic molecule from dehydrative cyclization [8]. However, the analogous results
361 with MHC II tetramers argue that the enhanced antigen presentation associated with monomer
362 delivery is not simply attributable to increased stability as peptide antigens are more stable.
363 Therefore, we think it more likely that the monomer delivery enhances the efficiency of
364 presentation by improving another aspect of antigen processing or presentation.

365 Our efforts to identify the molecular mechanism that enables transfer of the antigenic ligand
366 from the soluble MR1 to the cellular MR1 show that this process is dependent on actin dynamics
367 and enhanced if cellular MR1 is pre-loaded with 6-FP. Peptide editing on MHC I and MHC II
368 depends on the relative affinities of the available ligands and their competition for transiently
369 ligand-receptive antigen presenting molecules [3, 4, 33]. In line with this concept, we propose
370 that the endosomal compartment is a uniquely suited place for MR1 ligand exchange by virtue
371 of its high local concentration of antigens derived from internalized pathogens relative to the cell
372 as a whole. This enrichment of otherwise low abundance ligands may drive the equilibrium from
373 pre-bound ligands to internalized antigens specifically in endosomal compartments.

374 This analogy breaks down, however, in that peptides are not covalently bound to their antigen
375 presenting molecules. By contrast, a covalent bond needs to be broken in our exchange assay to
376 release the antigenic ligand from the soluble MR1. The Schiff base that anchors both 6-FP and 5-
377 OP-RU to the MR1 binding groove is considered labile under acidic conditions [6, 14].
378 Nevertheless, our results suggest that ligand exchange on MR1 does not require endosomal
379 acidification. Indeed, plate-bound MR1 was resistant to conformational changes associated with
380 ligand release under acidic conditions. This is in striking contrast to MR1-mediated presentation
381 of fixed whole *E.coli* [13] and the 5-A-RU pro-drug [12]. While the latter was designed to require
382 acidic conditions for release, the first suggests that the molecular mechanisms for MR1 loading
383 differ between *E.coli* and 5-OP-RU-loaded monomer. Importantly, *Mycobacterium tuberculosis* is

384 known to prevent endosomal acidification to evade immune recognition [45], making antigen
385 loading mechanisms that function at higher pH desirable. Alternatively, ligand transfer after
386 monomer delivery may be insensitive to bafilomycin because it occurs in the ER. Previous studies
387 have demonstrated that whole proteins from the extracellular environment can be imported into
388 this compartment [46-48], so this may be true for the MR1 monomer, too. In that case, we would,
389 however, expect monomer delivery to efficiently supply ligand to MHC I molecules as well, which
390 was not the case (Figure 5c). Our BFA experiments also show that MR1 ligand exchange can take
391 place after MR1 is released from the ER bound to 6-FP (Figure 5g).

392 While the molecular mechanism and the subcellular location of ligand exchange remain to be
393 determined, our data lead us to propose that it is a facilitated process catalyzed by a yet
394 unidentified exchange chaperone (Supplementary Figure 9). Monomer delivery may increase the
395 efficiency of exchange by enhancing the interaction between pre-loaded MR1 and this
396 chaperone. Indeed, specific chaperones facilitate the release of pre-loaded ligands, stabilize the
397 transiently unoccupied antigen presenting molecule, and mediate the re-loading with antigenic
398 cargo in other examples of ligand exchange. For MHC I, for instance, this function can be fulfilled
399 by TAPBPR in the Golgi (reviewed e.g. in [49] and [50]). For MHC II, HLA-DM chaperones
400 endosomal ligand exchange and exchange kinetics are further modulated by its regulator HLA-
401 DO (recently reviewed in [33] and [4]). Recent screens for modulators of MR1 loading and
402 trafficking have identified numerous interaction partners through both genetic techniques and
403 protein co-immunoprecipitation [7, 51]. These studies found MR1-mediated antigen
404 presentation to be regulated by tapasin and TAPBPR [7, 34] and the P5-type ATPase ATP13A1
405 [51], but have largely focused on ER and Golgi-resident proteins. Discovery approaches more
406 specifically targeted at interaction partners during ligand exchange in endosomal compartments
407 may be needed to identify the chaperone(s) involved in this process.

408 In this manuscript, we explored the mechanisms by which MR1 ligands can be delivered
409 exogenously using MR1 itself to stabilize an inherently unstable ligand. This mode of ligand
410 delivery is a powerful tool to identify chaperones involved in the re-loading of pre-loaded MR1
411 molecules which can then be tested for their involvement in physiological settings such as

412 mycobacterial infection. 5-OP-RU was also recently successfully used to boost mucosal immunity
413 in the context of vaccinations against respiratory pathogens [52]. Thus, in addition to its use in
414 exploring the molecular underpinnings of ligand exchange, we also postulate MR1/ligand
415 complexes could be used as an adjuvant or antigen delivery strategy in novel vaccination
416 approaches.

417 Methods

418 *Human subjects*

419 This study was conducted according to the principles expressed in the Declaration of Helsinki.
420 Study participants, protocols, and consent forms were approved by the Institutional Review
421 Board at Oregon Health & Science University (OHSU) (IRB00000186).

422 *Cells and bacteria*

423 *M. smegmatis* (strain mc^{2}155) supernatant was obtained by growing *M. smegmatis* and filtering
424 the supernatant as described previously [10]. PBMCs were isolated from whole blood obtained
425 by leukapheresis with informed consent, as previously described [53]. Human monocyte-derived
426 dendritic cells (DCs) were isolated from PBMCs by plate adherence and cultured in RPMI+10%
427 heat-inactivated human serum (HuS) with 30 ng/ml GM-CSF (Immunex) and 10 ng/ml IL-4 (R&D
428 Systems) as previously described [36]. BEAS-2B cells were obtained from the American Type
429 Culture Collection (ATCC) and cultured as recommended. BEAS-2B MR1$^{-/-}$, BEAS-2B MR1$^{-/-}$: MR1A
430 [20, 21] and the BEAS-2B cell line overexpressing GFP-tagged MR1A (BEAS-2B.MR1-GFP) [9] were
431 described previously. THP-1 cells were obtained from ATCC. THP-1 MR1$^{-/-}$ and THP-1 MR1$^{-/-}$: MR1
432 cell lines were described previously [21, 54]. The THP-1 MR1$^{-/-}$ from the Sewell lab constitutively
433 express Cas9 protein whereas the THP-1 MR1$^{-/-}$: MR1 cells from the Cerundolo lab do not. EBV-
434 transformed B cell lines (LCL) were generated in our laboratory using supernatants from the cell
435 line 9B5–8 (ATCC). A549 cells were obtained from ATCC. The MR1 R9H res construct was based
436 on [24]. MR1 res and MR1 R9H res contain silent mutations to make the sequence resistant to
437 CRISPR/Cas9 editing in the MR1$^{-/-}$ background. The coding sequence with a downstream IRES GFP
438 [55] was ordered from GeneArt (ThermoFisher) and cloned into our previously described pCI AscI

439 vector [10]. Plasmids were sequenced at the OHSU sequencing core and transfected into BEAS-
440 2B MR1$^{-/-}$ cells using the Amaxa nucleofection system with Kit T solution (Lonza). The transfection
441 efficiency was evaluated via GFP expression by flow cytometry (Supplementary Figure 3).
442 *Trichoplusia ni* (Hi-5) and *Spodoptera fugiperda* (Sf9) cells for baculovirus production and
443 recombinant protein expression were maintained as described previously [56].

444 *CRISPR/Cas9-mediated knock out of STX4*

445 Early passage BEAS-2B WT cells were stably transduced with lentiviral particles encoding Cas9 by
446 spinoculation as previously described [57]. Transduced cells were selected by culturing with 5
447 µg/ml Blasticidin (Life Tech) for 12 days. Three sgRNA constructs targeting STX4 were generated
448 and packaged into lentiviral particles as described [58]. Early passage BEAS-2B.Cas9 cells were
449 then transduced with supernatant containing these lentiviral particles in the presence of 200 µg
450 Polybrene (Sigma). Transduced cells were selected by culturing with 8 µg/ml Puromycin (Sigma)
451 for 6 days. Monoclonal populations were created by limiting dilution and a functional screen was
452 performed by ELISPOT. Genomic editing efficiency and clonality were verified by Sanger
453 sequencing. Briefly, DNA was isolated from STX4 KO clones and BEAS-2B.Cas9 control cells using
454 the QIAamp DNA Micro Kit (Qiagen) per manufacturer's protocols. DNA surrounding the sgRNA
455 target site was amplified by PCR and purified using the QIAquick PCR Purification Kit (Qiagen) per
456 manufacturer's protocols. Sanger sequencing was performed by capillary electrophoresis at the
457 OHSU Vollum Institute DNA Sequencing Core and sequences were analyzed by TIDE [59] and ICE
458 [60]. Sequence of the sgRNA used to generate the STX4 KO clonal cell line used in this manuscript:
459 AGAACGTGGAGCGGATTCGG.

460 *T cell clones*

461 All T cell clones were expanded and maintained as previously described [19, 26]. Three T cell
462 clones were used in this work. Two clones have been published previously (D426-G11 [15, 19]
463 and D480-F6 [26, 27]). D481-D1 is a CD4^{+} T cell clone that recognizes Esat6$_{73-87}$. This clone was
464 generated in a limiting dilution assay by adding either 100, 200 or 600 CD4^{+} T cells (CD4
465 microbeads, Miltenyi) isolated from PBMC from D481, a participant who had active tuberculosis,
466 to wells of a 96 well plate containing 1e5 irradiated (3,500 rad using a Cs source) allogeneic

467 PBMCs, 1e4 irradiated (3,500 rad using a Cs source) autologous dendritic cells (prepared as
468 described above), 2 µg/ml Esat6 protein (BEI Resources), 5 ng/ml interleukin-2 (Proleukin) and
469 incubated at 37°C for two weeks. Wells with growth were assessed for response to an Esat6
470 peptide pool consisting of 15mers overlapping by 11 amino acids in an IFN-γ ELISPOT. T cell
471 clones that responded to the Esat6 peptide pool were expanded as described previously [19, 26]
472 and further screened against the individual 15mers. The restricting allele is not known for this
473 clone, but D481 expresses these class II alleles: DRB1*08:01, DRB1*13:01, DPB1*01:01,
474 DPB1*04:01, DQB1*04:02 and DQB1*06:03 (HLA typing by Kashi Clinical Laboratories, Portland,
475 OR).

476 *ELISPOT assays*

477 For the plate-bound tetramer ELISPOT (tetraSPOT) assay, ELISPOT plates were coated with an
478 anti–IFN-γ antibody, as previously described [61]. At the time of coating, MR1/5-OP-RU and
479 MR1/6-FP tetramers conjugated to PE obtained from the NIH tetramer core [8] were added at a
480 range of concentrations. After overnight incubation at 4°C, ELISPOT plates were washed three
481 times with phosphate-buffered saline and then blocked with RPMI 1640 + 10% human serum
482 (RPMI+10% HuS) for at least 1 h. T cell clones (1e3-2e4) were added to wells overnight. IFN-γ
483 ELISPOTs were enumerated following development as previously described [61]. For all other
484 ELISPOT assays, ELISPOT plates were coated with anti-IFN-γ antibody and blocked as described
485 above. 1e4 DC, LCL, THP-1 or BEAS-2B cells were plated in the ELISPOT wells in RPMI+10% HuS.
486 Tetramer, monomer, ligand or peptide were added to the wells at concentrations indicated for
487 each experiment. PHA was used as positive control. After at least 1 h, 1e3-2e4 T cell clones were
488 added and the plate was incubated overnight at 37°C. 6-FP pre-treatment assays were performed
489 as described [10]. Briefly, BEAS-2B.MR1-GFP cells were plated in 6-well tissue culture plates and
490 treated with 6-FP *vs* NaOH control over night. On the next day, the cells were harvested and used
491 as APCs in an IFN-γ ELISPOT assay as described above. For experiments with Bafilomycin A1
492 (BAFA1, MedChemExpress), BEAS-2B cells were incubated with BAFA1 for 2 h at indicated
493 concentrations prior to the addition of 100 pM MR1/5-OP-RU monomer or 50 nM 5-OP-RU
494 prodrug (MedChemExpress) in an IFN-γ ELISPOT assay as described above.

495 *5-OP-RU Ligand*

496 5-(2-oxopropylideneamino)-6-d-ribitylaminouracil (5-OP-RU) was made from two sources of 5-
497 amino-6-D-ribitylaminouracil (5-A-RU). For the first method, 5-nitro-6-d-ribitylaminouracil (5-N-
498 RU) was prepared by the OHSU Medicinal Chemistry Core. 5-A-RU was freshly prepared from 5-
499 N-RU following a previously described procedure [8]. In brief, 4.8 mg of 5-N-RU was dissolved in
500 400 µl of 50 mM MES, pH 5.8. 8-fold molar excess of sodium dithionite powder was added and
501 incubated in the dark at 90°C for five minutes under argon. The solution was chilled in an ice
502 water bath. To prepare 5-OP-RU, at least 15 molar equivalents of methylglyoxal was added to 5-
503 A-RU in 100 mM HEPES, pH 7.2, 150 mM NaCl to give a stock solution at 20 mM. For the second
504 method, 5-A-RU*HCl was prepared by the OHSU Medicinal Chemistry Core following a previously
505 described procedure [62]. To prepare 5-OP-RU, equal volumes of circa 650 mM methylglyoxal
506 (Sigma) and 32 mM 5-A-RU*HCl dissolved in water were combined immediately before addition
507 to the assay to give a stock solution of 16 mM of 5-OP-RU. Mass spectrometry analysis confirmed
508 near-complete conversion of 5-A-RU into 5-OP-RU under similar conditions (Supplementary
509 Figure 8). For this, samples were directly injected into an AB Sciex TripleTOF 5600 quadrupole
510 time of flight mass spectrometer using the built-in syringe pump through a Hamilton Model 1710
511 N 100 µl syringe. Samples passing through the syringe were ionized by a PicoView ion source by
512 New Objective before passing through a Co-Ann technologies 11cm 20 µm inner diameter pulled
513 glass emitter which tapered to a 10 µm inner diameter at the tip. A stock solution of 32 mM 5-A-
514 RU was diluted 1:10 before injection into the mass spectrometer. 5-OP-RU was produced by
515 combining a 5 µl stock solution of 32 mM of 5-A-RU with a 5 µl 1:10 dilution from a 6.5 M stock
516 solution of methylglyoxal (Sigma). This 5-OP-RU was then diluted 1:10 for injection into the mass
517 spectrometer. Samples were examined in negative ion mode with the source voltage set at -2600
518 V. MS1 and MS2 data was acquired using Analyst 1.8 in manual tuning mode, with a TOF mass
519 range of 30 to 500 Da after 1 minute. MS2 data was collected in high sensitivity mode with a
520 declustering potential of -40 and a collision energy of -30 for 5-A-RU and -38 for 5-OP-RU. Data
521 was analyzed using PeakView 1.2.

522 *Flow Cytometry assays*

523 The following reagents were obtained through the NIH Tetramer Core Facility: MR1/5-OP-RU
524 tetramer and monomer and MR1/6-FP tetramer and monomer, HLA*B08:01/CFP10$_{3-11}$ tetramer,
525 HLA-DRB1*14:03/Esat6$_{73-87}$ tetramer, HLA-DRB1*14:03/control tetramer. Identification of MAIT
526 cells with MR1 tetramers was described in [8]. The D426-G11 TCR tetramer was made as specified
527 below. To confirm the specificity of the TCR tetramer as a staining reagent, BEAS-2B.MR1-GFP
528 cells were incubated with the indicated concentrations of 5-OP-RU or 6-FP, or the equivalent
529 volume of 0.01 M NaOH overnight. Cells were harvested with Trypsin and split into three wells
530 of a U-bottom 96-well plate each for staining with TCR tetramer, anti-MR1 antibody 26.5
531 (BioLegend, 361108), or isotype control antibody (BioLegend, 400222) for at least 30 min on ice.
532 BEAS-2B MR1-/- cells transfected with the MR1 res or MR1 R9H res plasmids were analyzed
533 similarly. For ligand titration experiments, 5e4 BEAS-2B.MR1-GFP cells per well were incubated
534 with the indicated concentrations of free 5-OP-RU or MR1/5-OP-RU monomer in a 24-well plate
535 overnight. Cells were harvested with Trypsin, transferred to a 96-well U-bottom plate, washed,
536 and stained with TCR tetramer for at least 30 min at 4° C. For time course experiments, 5e4 BEAS-
537 2B.MR1-GFP cells per well were plated in 24-well plates. Free 5-OP-RU or MR1/5-OP-RU were
538 added to the indicated final concentrations for the indicated amounts of time. Samples from all
539 time points were harvested and stained at the same time as above. Free ligand and monomer
540 titrations were performed in parallel in both sets of experiments. For the actin blockade, 5e4
541 BEAS-2B.MR1-GFP cells were plated in 24-well plates and left to adhere overnight. Cells were
542 then treated with 10 µM Latrunculin B (Sigma) or the equivalent volume of DMSO (Sigma). After
543 1 h, MR1/5-OP-RU or MR1/6-FP monomer was added to a final concentration of 100 nM and the
544 cells were incubated for another 4 h before staining as above. For Brefeldin A blocking
545 experiments, BEAS-2B.MR1-GFP cells were incubated with 94 µM 6-formylpterin (6-FP, Schircks)
546 or the equivalent volume of 0.01 M NaOH (Sigma) overnight at 37°C at 5e4/well in a 24-well plate.
547 6-FP was washed off and the cells treated with 50 µg/ml Brefeldin A (BFA, Sigma) or the
548 equivalent volume of DMSO (Sigma) for 1 h, followed by the addition of MR1/6-FP or MR1/5-OP-
549 RU monomer (100 nM) or free 5-OPRU (5 µM) or 6-FP (100 µM) and incubation at 37°C for 4 h.
550 Cells were then stained with TCR tetramer as above. The gating strategy is shown in

551 Supplementary Figure 10. TCR tetramer was used at 150 or 300 nM. BEAS-2B WT cells were used
552 for unstained and single color controls. Anti-MHC I antibody W6/32 (BioLegend, 311410) was
553 used for the APC single color control due to low MR1 expression on BEAS-2B WT cells. For surface
554 staining of BEAS-2B.MR1-GFP cells with streptavidin, 3e5 cells were incubated with 50 nM of
555 MR1/5-OP-RU monomer or medium overnight. These cells were split into multiple wells and
556 either stained with the TCR tetramer as described above or blocked with PBS + goat, human, and
557 bovine serum for at least 30 min on ice and then stained with Streptavidin-APC (Agilent) for 40
558 min on ice or with biotinylated anti-MR1 antibody 26.5 for 40 minutes on ice, followed by
559 Steptavidin-APC for 40 minutes on ice. For tetramer staining of the CD8 T cell clone D480-F6, 1e5
560 T cell clones were incubated with the HLA*B08:01/CFP10$_{3-11}$ tetramer at 1:500 (0.127 µg/well)
561 for 45 minutes at 37°C. For tetramer staining of the CD4 T cell clone D481-D1, 1e5 T cell clones
562 were incubated with the HLA-DRB1*14:03/Esat6$_{73-87}$ or HLA-DRB1*14:03/control at 6 µg/ml for
563 1 h at 37°C. Cells were subsequently stained with an antibody cocktail containing LIVE/DEAD
564 Fixable Dead Cell Stain Kit (Thermo Fisher), and surface stained with the antibodies to CD4 (BD
565 Biosciences, clone SK3 348789), CD8 (Biolegend, clone SK1344714), and CD3 (BD Biosciences,
566 clone SK7340663), for 30 minutes at 4°C. Samples were washed and fixed with 1% PFA.
567 Acquisition was performed using a BD FACSymphony, LSRII, or Canto cytometer. The gating
568 strategy is shown in Supplementary Figure 11. Flow cytometric analysis was performed using
569 FlowJo version 10.6.1 or 10.7.1 (Treestar, Ashland, OR, USA). Plots show GFP+ gates to ensure
570 only cells over-expressing MR1 are included in the analysis.

571 *Knock down of candidate chaperones*

572 For siRNA-mediated knock down of candidate chaperones, siRNAs targeting TAPBPR (Assay ID
573 s229969), tapasin (Assay ID 41850), or AP2A1 (Assay ID s183) or a missense control (4390844)
574 (all Thermo Fisher Scientific) were nucleofected into 1e6 BEAS-2B WT cells at 300 nM according
575 to the manufacturer's instructions (Lonza, Nucleofector Kit T). Cells were allowed to rest
576 overnight (TAPBPR and tapasin) or two days (AP2A1) before use in an ELISPOT assay as
577 described above. RNA levels of targeted transcripts were measured by qRT PCR at the time of
578 ELISPOT using Taqman probes Hs00794155_m1, Hs00917451_g1, and Hs00900330_m1 with

579 GAPDH (Hs02758991_g1) as the housekeeping gene (all Thermo Fisher Scientific). For AP2A1,
580 equal cell numbers were also lysed in Lysis Buffer (Chromotek) with Protease Inhibitor cocktail
581 (Roche) at the time of ELISPOT and lysates of all three experiments were analyzed together by
582 Western blot. Briefly, lysates were combined with Loading Buffer and Reducing Agent (both
583 Invitrogen), separated on 4-20% polyacrylamide gels (Bio-Rad), and transferred onto PVDF
584 membrane (Millipore). The membrane was blocked with Blocking Buffer (Odyssey) for 1 h at
585 room temperature before incubation with mouse anti-AP2A1 (BD, 610501) and rabbit anti-
586 ACTB (Abcam, ab8227) primary antibodies overnight at 4° C. The blot was developed with LI-
587 COR IRDye secondary antibodies (goat anti-mouse 800CW and goat anti-rabbit 680RD) and
588 imaged simultaneously on an Odyssey imager.
589
590 *Recombinant protein expression and purification*
591 All experiments using MR1 monomer and tetramer were performed with the reagent(s)
592 provided by the NIH Tetramer Core Facility (NTCF). Recombinant DP10.7 γδ TCR and HLA-
593 A2/MART-1 peptide used as controls in the ELISA were produced as previously described [63,
594 64]. The D426-G11 TCR was produced as previously described for other MAIT TCRs [65]. Briefly,
595 the D426-G11 TCR V(D)J region of each TCR chain was cloned separately into the pAcGP67a
596 vector after the GP67 signal sequence and before either a “cysteine-optimized” TRAC or TRBC
597 sequence [66]. To ensure heterodimer formation, the chains were tagged with cleavable C-
598 terminal acidic and basic zippers [67] each followed with a 6xHis tag. The alpha chain construct
599 contained a C-terminal AviTag before the zipper cleavage site. The P1 and P2 baculoviruses
600 were produced in Sf9 cells [56], then the baculoviruses were added in tandem to Hi-5 cells and
601 the cells were allowed to express the recombinant protein for 72 h. The supernatant was
602 harvested and the protein purified by Ni-NTA chromatography. Recombinant TCR was then
603 treated with recombinant HRV 3C protease overnight and the cleaved zippers were removed
604 with Ni-NTA. The protein was biotinylated *in vitro* using recombinant BirA ligase and the
605 biotinylation efficiency checked by a streptavidin gel-shift assay. Finally, it was purified by size
606 exclusion chromatography and tetramerized with streptavidin-APC (Agilent). This reagent is

607 available upon request after the completion of an MTA that includes a clear description of how
608 the material would be used.

609 *Microscopy*

610 BEAS-2B cells (1e5) were seeded on a chamber slide and incubated for 18 h at 37C. MR1/5-OP-
611 RU tetramer conjugated to AF647 (200 nM) was added to the experimental wells for 2 h at RT.
612 Control wells received no tetramer. To determine whether the tetramer was observed in the
613 cells, CellMask Orange Plasma (1:5000 dilution, Invitrogen) was added for 10 min. To examine
614 whether the tetramer localized to endosomal compartments, CellLight reagents (Thermofisher)
615 for early endosomes (Rab5) or lysosomes (LAMP1) were added for 18 h prior to addition of the
616 tetramer. For all imaging, DAPI was added during PBS washes, and cells were fixed prior to data
617 acquisition. Images were acquired on a Keyence BZ-X810 Fluorescence microscope or high-
618 resolution wide-field CoreDV microscope (Applied Precision) with CoolSNAP ES2 HQ (Nikon),
619 using nuclear staining with DAPI to identify un-biased fields of view. Localization of the tetramer
620 to endosomal compartments was quantified using Imaris image analysis software as previously
621 described [36].

622 *Cell-free acidification assay*

623 In addition to MR1/5-OP-RU and MR1/6FP from the NIH Tetramer Core, recombinant,
624 biotinylated γδ TCR ("DP10.7") [63] and HLA-A2:MART-1 [64] were made in-house as previously
625 described and used as controls for this ELISA assay. Extensive washing with PBS pH 7.4 + 0.5%
626 Tween-20 was performed between each step/treatment outlined below. First, traptavidin, a
627 variant of streptavidin with a slower biotin off-rate [68], was immobilized on an ELISA plate in 0.1
628 M Na_2CO_3, pH 9.6 overnight. The plate was blocked with 0.5% BSA in 1xPBS, then biotinylated
629 MR1, TCR, and HLA-A2 were immobilized as appropriate. Eight working buffers of 1xPBS were
630 made from a house-made 10xPBS stock spanning pH 4.6-7.4. Protein was treated with either PBS
631 pH 7.4 (controls) or PBS of variable pH overnight at 4°C. (This experiment was also performed
632 with a citrate-phosphate buffer system, which unlike PBS, has a buffering range spanning the
633 experimental conditions, and the results did not differ from those using PBS, which has a
634 buffering range of ~5.8-7.4 pH units.) After removal of the acidic buffer and washing with PBS pH

635 7.2, either anti-human MR1 (unlabeled, clone 26.5, BioLegend 361102) or anti-human β_2m
636 (unlabeled, clone B2M-01, Novus Biologicals NB500-317) antibody was applied to the plate,
637 followed by a rabbit anti-mouse IgG H+L, HRP-conjugated secondary antibody (Abcam ab6728).
638 The ELISA was developed with a TMB substrate kit (Thermo Scientific 34021) and the absorbance
639 was detected at 450 nm using a Tecan Safire 2 plate reader.

640 *Data analysis and Statistics*

641 Data were analyzed with Prism 9 GraphPad Software. For measurements of functional avidity,
642 curves were determined by non-linear regression and best-fit EC_{50} was calculated. EC_{50} values
643 were compared with the extra sum-of-squares F test.

644 Data Availability

645 The authors declare that the data supporting the findings of this study are available within the
646 paper and its supplementary information files.

647 Acknowledgements

648 We would like to thank the participants who gave time and dedication to this health research as
649 well as Erin Merrifield, Department of Pediatrics, OHSU, for her contributions to this study. We
650 also thank Sobhan Roy and Mayuri Viswanathan for kindly providing recombinant γδ TCR and
651 HLA-A2 for use in this study.

652 This project has been funded in whole or in part with Federal funds from the National Institutes
653 of Allergy and Infectious Diseases, National Institutes of Health, Department of Health and
654 Human Services, under grant no AI147954 (EA, DML, WHH), AI134790 (DML), GM007183 (NAL),
655 AI129976 (MH), 1R01AI141549 (FT) and AI165618 (AO). This work was also supported in part by
656 Merit Award #I01 CX001562 from the U.S. Department of Veterans Affairs Clinical Sciences
657 Research and Development Program (MJH), Merit Award #I01 BX000533 from the U.S.
658 Department of Veterans Affairs Biomedical Laboratory (DML).

659 ## Author Contributions

660 CK, GS, NAL, DAL, EJA, DML and MH contributed to the conception and/or design of the work. CK
661 and GS are joint first authors. DML and MH jointly supervised the work. MC, MN, DAL and DML
662 contributed to clinical activities. AO, WHH, FT, EJA, DML and MH raised grants to fund the
663 research. CK, GS, NAL, MC, MN, AW, CL, TA, JB, TNL, CMH, MEH, JK, LA, AO, WHH, SM, FT, DAL,
664 EJA, DML and MH substantially contributed to the acquisition, analysis, or interpretation of data
665 and drafting of the manuscript. All authors substantially contributed to revising and critically
666 reviewing the manuscript for important intellectual content. All authors approved the final
667 version of this manuscript to be published and agree to be accountable for all aspects of the
668 work.

669 ## References

670 1. Crowther, M.D. and A.K. Sewell, *The burgeoning role of MR1-restricted T-cells in infection,*
671 *cancer and autoimmune disease.* Curr Opin Immunol, 2021. **69**: p. 10-17.
672 2. Hinks, T.S.C. and X.W. Zhang, *MAIT Cell Activation and Functions.* Front Immunol, 2020. **11**:
673 p. 1014.
674 3. Trowitzsch, S. and R. Tampé, *Multifunctional Chaperone and Quality Control Complexes in*
675 *Adaptive Immunity.* Annual Review of Biophysics, 2020. **49**(1): p. 135-161.
676 4. Alvaro-Benito, M. and C. Freund, *Revisiting nonclassical HLA II functions in antigen*
677 *presentation: Peptide editing and its modulation.* HLA, 2020. **96**(4): p. 415-429.
678 5. Moody, D.B. and R.N. Cotton, *Four pathways of CD1 antigen presentation to T cells.* Curr
679 Opin Immunol, 2017. **46**: p. 127-133.
680 6. McWilliam, H.E., et al., *The intracellular pathway for the presentation of vitamin B-related*
681 *antigens by the antigen-presenting molecule MR1.* Nat Immunol, 2016. **17**(5): p. 531-7.
682 7. McWilliam, H.E.G., et al., *Endoplasmic reticulum chaperones stabilize ligand-receptive MR1*
683 *molecules for efficient presentation of metabolite antigens.* Proc Natl Acad Sci U S A, 2020.
684 **117**(40): p. 24974-24985.
685 8. Corbett, A.J., et al., *T-cell activation by transitory neo-antigens derived from distinct*
686 *microbial pathways.* Nature, 2014. **509**(7500): p. 361-5.
687 9. Harriff, M.J., et al., *Endosomal MR1 Trafficking Plays a Key Role in Presentation of*
688 *Mycobacterium tuberculosis Ligands to MAIT Cells.* PLoS Pathog, 2016. **12**(3): p. e1005524.
689 10. Karamooz, E., et al., *MR1 recycling and blockade of endosomal trafficking reveal*
690 *distinguishable antigen presentation pathways between Mycobacterium tuberculosis*
691 *infection and exogenously delivered antigens.* Scientific Reports, 2019. **9**(1): p. 4797.
692 11. Kulicke, C., et al., *Covering All the Bases: Complementary MR1 Antigen Presentation*
693 *Pathways Sample Diverse Antigens and Intracellular Compartments.* Frontiers in
694 Immunology, 2020. **11**.

695 12. Lange, J., et al., *The Chemical Synthesis, Stability, and Activity of MAIT Cell Prodrug Agonists*
696 *That Access MR1 in Recycling Endosomes.* ACS Chemical Biology, 2020.
697 13. Ussher, J.E., et al., *TLR signaling in human antigen-presenting cells regulates MR1-*
698 *dependent activation of MAIT cells.* European Journal of Immunology, 2016. **46**(7): p. 1600-
699 1614.
700 14. McWilliam, H.E.G. and M. Salio, *Understanding and modulating the MR1 metabolite*
701 *antigen presentation pathway.* Molecular Immunology, 2021. **129**: p. 121-126.
702 15. Harriff, M.J., et al., *MR1 displays the microbial metabolome driving selective MR1-restricted*
703 *T cell receptor usage.* Sci Immunol, 2018. **3**(25).
704 16. Mak, J.Y., et al., *Stabilizing short-lived Schiff base derivatives of 5-aminouracils that activate*
705 *mucosal-associated invariant T cells.* Nat Commun, 2017. **8**: p. 14599.
706 17. Priya, R. and R.R. Brutkiewicz, *MR1 Tetramer-Based Artificial APCs Expand MAIT Cells from*
707 *Human Peripheral Blood That Effectively Kill Glioblastoma Cells.* Immunohorizons, 2021.
708 **5**(6): p. 500-511.
709 18. Cruz, F.M., A. Chan, and K.L. Rock, *Pathways of MHC I cross-presentation of exogenous*
710 *antigens.* Semin Immunol, 2023. **66**: p. 101729.
711 19. Gold, M.C., et al., *Human mucosal associated invariant T cells detect bacterially infected*
712 *cells.* PLoS Biol, 2010. **8**(6): p. e1000407.
713 20. Narayanan, G.A., et al., *Alternative splicing of MR1 regulates antigen presentation to MAIT*
714 *cells.* Sci Rep, 2020. **10**(1): p. 15429.
715 21. Salio, M., et al., *Ligand-dependent downregulation of MR1 cell surface expression.* Proc Natl
716 Acad Sci U S A, 2020. **117**(19): p. 10465-10475.
717 22. Lion, J., et al., *MR1B, a natural spliced isoform of the MHC-related 1 protein, is expressed*
718 *as homodimers at the cell surface and activates MAIT cells.* Eur J Immunol, 2013. **43**(5): p.
719 1363-73.
720 23. Salerno-Goncalves, R., T. Rezwan, and M.B. Sztein, *B cells modulate mucosal associated*
721 *invariant T cell immune responses.* Front Immunol, 2014. **4**: p. 511.
722 24. Howson, L.J., et al., *Absence of mucosal-associated invariant T cells in a person with a*
723 *homozygous point mutation in MR1.* Sci Immunol, 2020. **5**(49).
724 25. Eckle, S.B., et al., *A molecular basis underpinning the T cell receptor heterogeneity of*
725 *mucosal-associated invariant T cells.* J Exp Med, 2014. **211**(8): p. 1585-600.
726 26. Lewinsohn, D.A., et al., *Immunodominant tuberculosis CD8 antigens preferentially*
727 *restricted by HLA-B.* PLoS Pathog, 2007. **3**(9): p. 1240-9.
728 27. Lancioni, C., et al., *Recognition of CD8(+) T-cell epitopes to identify adults with pulmonary*
729 *tuberculosis.* Eur Respir J, 2019. **53**(5).
730 28. Adams, S., et al., *HLA class I and II genotype of the NCI-60 cell lines.* J Transl Med, 2005.
731 **3**(1): p. 11.
732 29. Le Bourhis, L., et al., *Antimicrobial activity of mucosal-associated invariant T cells.* Nat
733 Immunol, 2010. **11**(8): p. 701-8.
734 30. Huang, S., et al., *Evidence for MR1 antigen presentation to mucosal-associated invariant T*
735 *cells.* J Biol Chem, 2005. **280**(22): p. 21183-93.
736 31. Kjer-Nielsen, L., et al., *MR1 presents microbial vitamin B metabolites to MAIT cells.* Nature,
737 2012. **491**(7426): p. 717-23.

32. Bowman, E.J., A. Siebers, and K. Altendorf, *Bafilomycins: a class of inhibitors of membrane ATPases from microorganisms, animal cells, and plant cells.* Proc Natl Acad Sci U S A, 1988. **85**(21): p. 7972-6.
33. Sadegh-Nasseri, S., *Partnering for the major histocompatibility complex class II and antigenic determinant requires flexibility and chaperons.* Curr Opin Immunol, 2021. **70**: p. 112-121.
34. McShan, A.C., et al., *TAPBPR employs a ligand-independent docking mechanism to chaperone MR1 molecules.* Nat Chem Biol, 2022. **18**(8): p. 859-868.
35. Lim, H.J., et al., *A specialized tyrosine-based endocytosis signal in MR1 controls antigen presentation to MAIT cells.* J Cell Biol, 2022. **221**(12).
36. Harriff, M.J., et al., *Human Lung Epithelial Cells Contain Mycobacterium tuberculosis in a Late Endosomal Vacuole and Are Efficiently Recognized by CD8+ T Cells.* PLOS ONE, 2014. **9**(5): p. e97515.
37. Scheller, R.H., *In search of the molecular mechanism of intracellular membrane fusion and neurotransmitter release.* Nat Med, 2013. **19**(10): p. 1232-5.
38. Spessott, W.A., et al., *Syntaxin 4 mediates endosome recycling for lytic granule exocytosis in cytotoxic T-lymphocytes.* Traffic, 2017. **18**(7): p. 442-452.
39. Kennedy, M.J., et al., *Syntaxin-4 defines a domain for activity-dependent exocytosis in dendritic spines.* Cell, 2010. **141**(3): p. 524-35.
40. Chatterjee Bhowmick, D., et al., *Conventional and Unconventional Mechanisms by which Exocytosis Proteins Oversee beta-cell Function and Protection.* Int J Mol Sci, 2021. **22**(4).
41. Black, H.L., et al., *Knockout of syntaxin-4 in 3T3-L1 adipocytes reveals new insight into GLUT4 trafficking and adiponectin secretion.* J Cell Sci, 2022. **135**(1).
42. Lamichhane, R. and J.E. Ussher, *Expression and trafficking of MR1.* Immunology, 2017. **151**(3): p. 270-279.
43. Karamooz, E., M.J. Harriff, and D.M. Lewinsohn, *MR1-dependent antigen presentation.* Seminars in Cell & Developmental Biology, 2018. **84**: p. 58-64.
44. Blander, J.M., *Regulation of the Cell Biology of Antigen Cross-Presentation.* Annu Rev Immunol, 2018. **36**: p. 717-753.
45. Kinsella, R.L., et al., *Perspectives and Advances in the Understanding of Tuberculosis.* Annu Rev Pathol, 2021. **16**: p. 377-408.
46. Ackerman, A.L., et al., *Access of soluble antigens to the endoplasmic reticulum can explain cross-presentation by dendritic cells.* Nat Immunol, 2005. **6**(1): p. 107-13.
47. Spooner, R.A., et al., *Retrograde transport pathways utilised by viruses and protein toxins.* Virol J, 2006. **3**: p. 26.
48. Mukhopadhyay, S. and A.D. Linstedt, *Retrograde trafficking of AB_5 toxins: mechanisms to therapeutics.* J Mol Med (Berl), 2013. **91**(10): p. 1131-41.
49. Hafstrand, I., A. Aflalo, and L.H. Boyle, *Why TAPBPR? Implications of an additional player in MHC class I peptide presentation.* Current Opinion in Immunology, 2021. **70**: p. 90-94.
50. Thomas, C. and R. Tampe, *MHC I assembly and peptide editing - chaperones, clients, and molecular plasticity in immunity.* Curr Opin Immunol, 2021. **70**: p. 48-56.
51. Kulicke, C.A., et al., *The P5-type ATPase ATP13A1 modulates major histocompatibility complex I-related protein 1 (MR1)-mediated antigen presentation.* J Biol Chem, 2022. **298**(2): p. 101542.

782 52. Pankhurst, T.E., et al., *MAIT cells activate dendritic cells to promote T(FH) cell differentiation*
783 *and induce humoral immunity.* Cell Rep, 2023. **42**(4): p. 112310.
784 53. Lewinsohn, D.M., et al., *Mycobacterium tuberculosis-reactive CD8+ T lymphocytes: the*
785 *relative contribution of classical versus nonclassical HLA restriction.* J Immunol, 2000.
786 **165**(2): p. 925-30.
787 54. Laugel, B., et al., *Engineering of Isogenic Cells Deficient for MR1 with a CRISPR/Cas9*
788 *Lentiviral System: Tools To Study Microbial Antigen Processing and Presentation to Human*
789 *MR1-Restricted T Cells.* J Immunol, 2016. **197**(3): p. 971-82.
790 55. Olive, A.J., et al., *Chlamydia trachomatis-induced alterations in the host cell proteome are*
791 *required for intracellular growth.* Cell Host Microbe, 2014. **15**(1): p. 113-24.
792 56. Murhammer, D.W.e., *Baculovirus and insect cell expression protocols*. Methods in
793 Molecular Biology. Vol. 388. 2007, Totowa, NJ: Humana Press.
794 57. Tafesse, F.G., et al., *Disruption of Sphingolipid Biosynthesis Blocks Phagocytosis of Candida*
795 *albicans.* PLoS Pathog, 2015. **11**(10): p. e1005188.
796 58. Thomas, S.T., et al., *Fetal Liver-Derived Alveolar-like Macrophages: A Self-Replicating Ex*
797 *Vivo Model of Alveolar Macrophages for Functional Genetic Studies.* Immunohorizons,
798 2022. **6**(2): p. 156-169.
799 59. Brinkman, E.K., et al., *Easy quantitative assessment of genome editing by sequence trace*
800 *decomposition.* Nucleic Acids Res, 2014. **42**(22): p. e168.
801 60. Conant, D., et al., *Inference of CRISPR Edits from Sanger Trace Data.* Crispr j, 2022. **5**(1): p.
802 123-130.
803 61. Heinzel, A.S., et al., *HLA-E-dependent presentation of Mtb-derived antigen to human CD8+*
804 *T cells.* J Exp Med, 2002. **196**(11): p. 1473-81.
805 62. Li, K., et al., *Synthesis, stabilization, and characterization of the MR1 ligand precursor 5-*
806 *amino-6-D-ribitylaminouracil (5-A-RU).* PLoS One, 2018. **13**(2): p. e0191837.
807 63. Luoma, A.M., et al., *Crystal structure of Vδ1 T cell receptor in complex with CD1d-sulfatide*
808 *shows MHC-like recognition of a self-lipid by human γδ T cells.* Immunity, 2013. **39**(6): p.
809 1032-42.
810 64. Benveniste, P.M., et al., *Generation and molecular recognition of melanoma-associated*
811 *antigen-specific human γδ T cells.* Sci Immunol, 2018. **3**(30).
812 65. López-Sagaseta, J., et al., *The molecular basis for Mucosal-Associated Invariant T cell*
813 *recognition of MR1 proteins.* Proc Natl Acad Sci U S A, 2013. **110**(19): p. E1771-8.
814 66. Boulter, J.M., et al., *Stable, soluble T-cell receptor molecules for crystallization and*
815 *therapeutics.* Protein Eng, 2003. **16**(9): p. 707-11.
816 67. Chang, H.C., et al., *A general method for facilitating heterodimeric pairing between two*
817 *proteins: application to expression of alpha and beta T-cell receptor extracellular segments.*
818 Proc Natl Acad Sci U S A, 1994. **91**(24): p. 11408-12.
819 68. Chivers, C.E., et al., *A streptavidin variant with slower biotin dissociation and increased*
820 *mechanostability.* Nat Methods, 2010. **7**(5): p. 391-3.
821

822 Figures

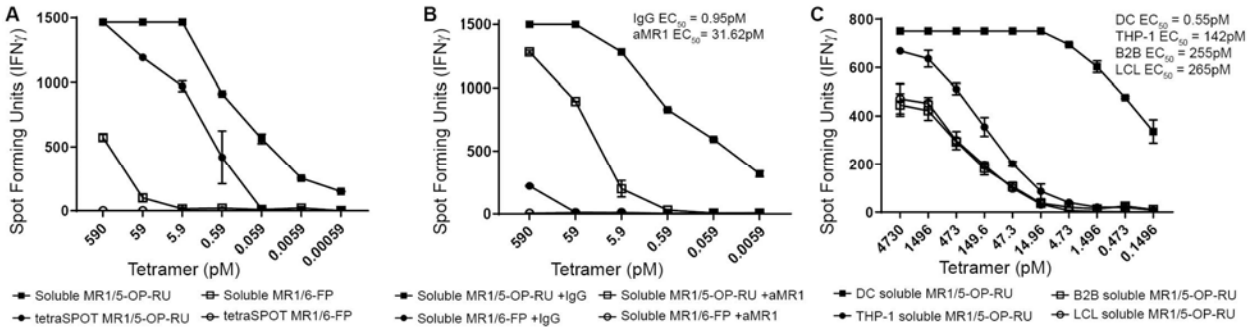

823
824 **Fig 1. MR1 ligands delivered to antigen presenting cells on soluble MR1 molecules are**
825 **efficiently recognized by MR1T cell clones. A.** MR1T cell clone (1e4) IFN-γ responses to MR1/5-
826 OP-RU or MR1/6-FP tetramer, either added to DCs (1e4) (exSPOT) or bound to ELISPOT plate
827 (tetraSPOT). **B.** MR1T cell clone (1e4) IFN-γ response to MR1/5-OP-RU is inhibited by anti-MR1
828 antibody blockade (2 µg/ml). **C**. MR1T cell clone (1e4) IFN-γ response to MR1/5-OP-RU tetramer,
829 added to either DCs, THP-1 cells, BEAS-2B (B2B) cells or B-LCL (1e4). EC_{50} calculated using non-
830 linear regression and the difference in the EC_{50} was statistically significant between the curves
831 ($p<0.0001$) by the extra sum-of-squares F test. Data are representative of three independent
832 experiments each. Error bars denote SD between technical duplicates within the representative
833 experiment shown. For EC_{50} values of replicate experiments see Supplementary Tables 1+2.
834
835
836
837
838
839
840
841
842
843
844
845
846
847
848
849
850

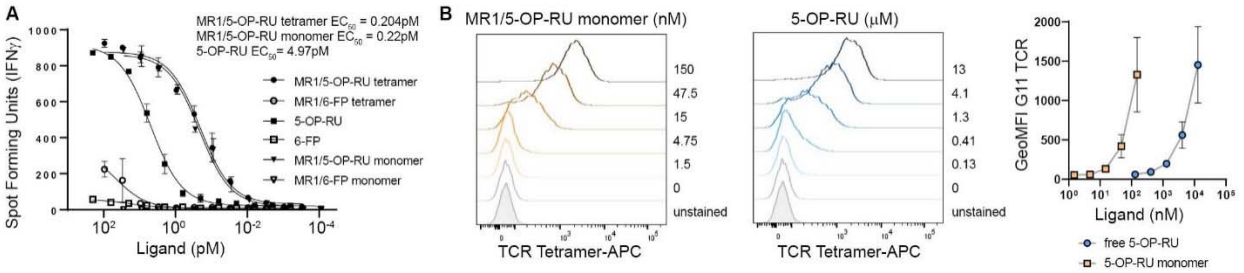

Fig 2. Ligand delivered in the context of MR1 monomer is presented more efficiently than free ligand. A. MR1T cell clone (1e4) IFN-γ response to DCs incubated with MR1/5-OP-RU tetramer, MR1/5-OP-RU monomer, and soluble 5-OP-RU. EC_{50} calculated using non-linear regression. The difference in the EC_{50} was statistically significant between the MR1/5-OP-RU tetramer and 5-OP-RU and between MR1/5-OP-RU monomer and 5-OP-RU curves ($p<0.0001$), but there was no significant difference in the EC_{50} of MR1/5-OP-RU tetramer and monomer by the extra sum-of-squares F test ($p=0.7486$). Data are representative of three independent experiments. Error bars denote SD between technical duplicates within the representative experiment shown. For EC_{50} values of replicate experiments see Supplementary Table 3. **B.** BEAS-2B.MR1-GFP cells were incubated with the indicated concentrations of MR1/5-OP-RU monomer or free 5-OP-RU overnight and surface stained for flow cytometry with APC-conjugated TCR tetramer. Representative histograms are shown on the left with pooled geometric mean fluorescence intensity from four experiments shown on the right. The same unstained and untreated control are shown in both histogram plots for easy comparison. Error bars denote SD.

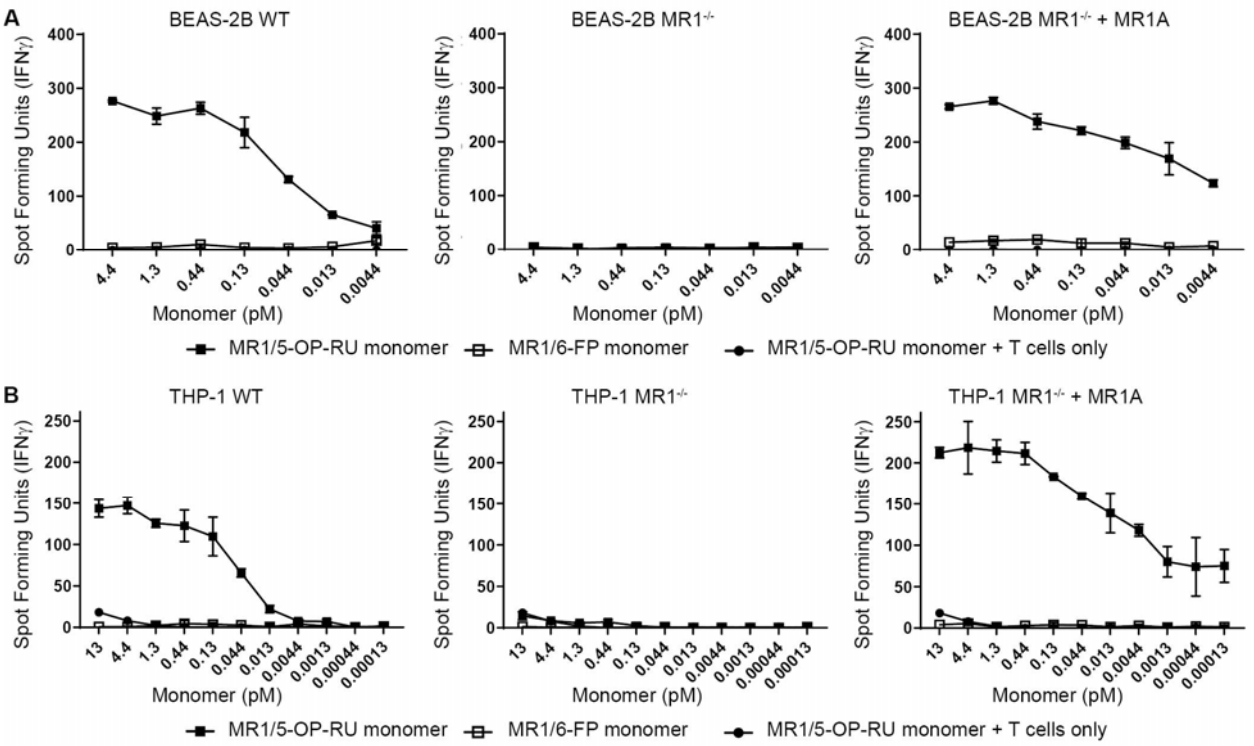

Fig 3. Presentation of MR1 ligands delivered on soluble MR1 molecules requires cellular MR1. **A.** MR1T cell clone (1e3) IFN-γ response to BEAS-2B, BEAS-2B MR1$^{-/-}$ and BEAS-2B MR1$^{-/-}$: MR1A (1e4) incubated with MR1/5-OP-RU or MR1/6-FP monomers. Also included MR1T clone IFN-γ response to MR1/5-OP-RU monomer only with no antigen presenting cells. **B.** Same as **A.**, except the antigen presenting cells are THP-1, THP-1 MR1$^{-/-}$ and THP-1 MR1$^{-/-}$: MR1A (1e4). Data are representative of two independent experiments. Error bars denote SD of technical duplicates within the representative experiments shown.

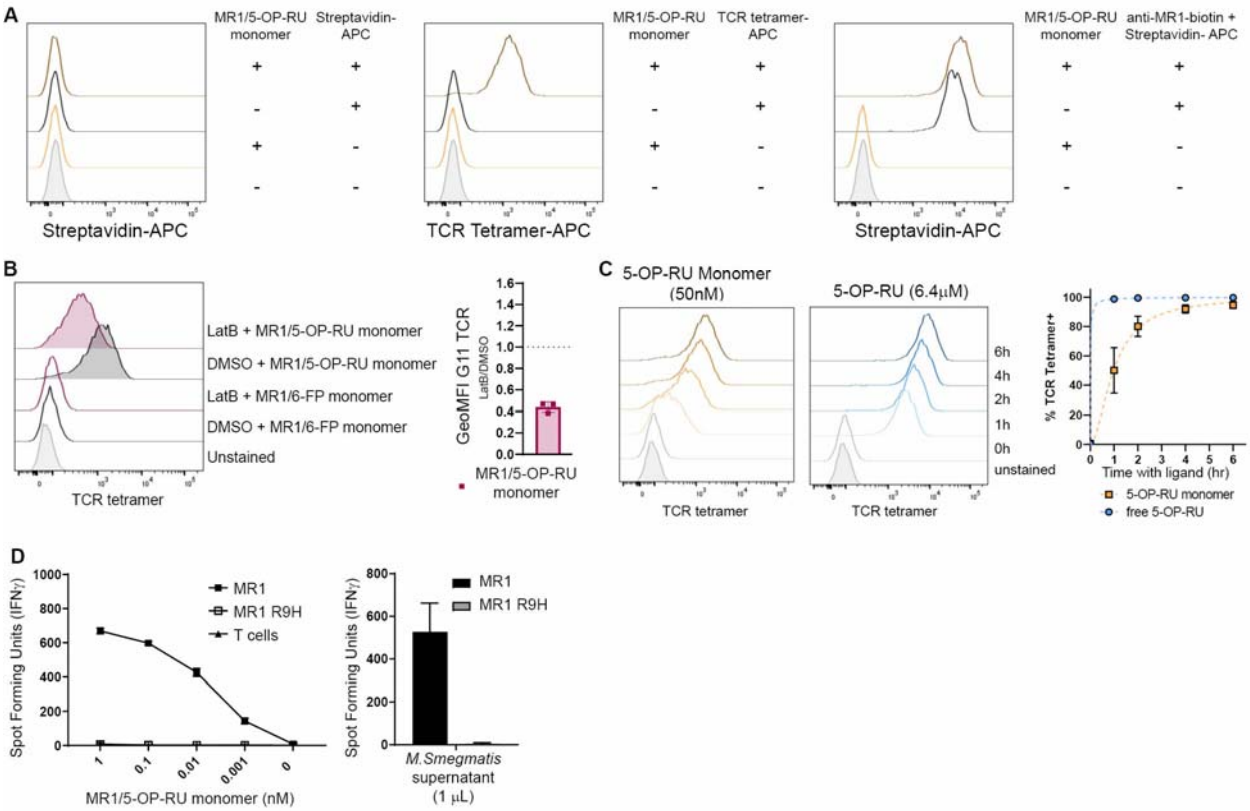

Fig 4. Ligands are transferred from the soluble MR1 molecules onto cellular MR1.
A. BEAS-2B.MR1-GFP cells (3e5) were pre-incubated with 50 nM of MR1/5-OP-RU monomer overnight before staining with either Streptavidin (left), TCR tetramer (middle) or biotinylated 26.5 anti-MR1 antibody followed by Streptavidin (right). The same unstained sample is shown in all panels and the same primary antibody only controls are shown in the left and right panels for easy comparison. Data are representative of three independent experiments. **B.** BEAS-2B.MR1-GFP cells were pre-incubated with 10 μM of latrunculin B (LatB) for 1 h before addition of MR1/5-OP-RU or MR1/6-FP monomer for an additional 4 h. Cells were surface stained with TCR tetramer. Representative histograms are shown on the left with pooled geometric mean fluorescence intensity from three experiments shown on the right. The same unstained and untreated control are shown in both histogram plots for easy comparison. Error bars denote SD. **C**. BEAS-2B.MR1-GFP cells were incubated with either 50 nM MR1/5-OP-RU monomer or 6.4 μM of free 5-OP-RU for indicated amounts of time before surface staining for flow cytometry with TCR tetramer. Representative histograms are shown on the left with pooled geometric mean fluorescence intensity from three experiments shown on the right. Error bars denote SD. **D.** MR1T cell clone (1e3) IFN-γ response to BEAS-2B MR1$^{-/-}$ cells (1e4) that had been transfected with the MR1 or MR1 R9H plasmid, followed by addition of the MR1/5-OP-RU monomer, or 1 μL of *M. smegmatis* supernatant. Data are representative of three independent experiments. Error bars denote SD between technical duplicates within the representative experiment shown.

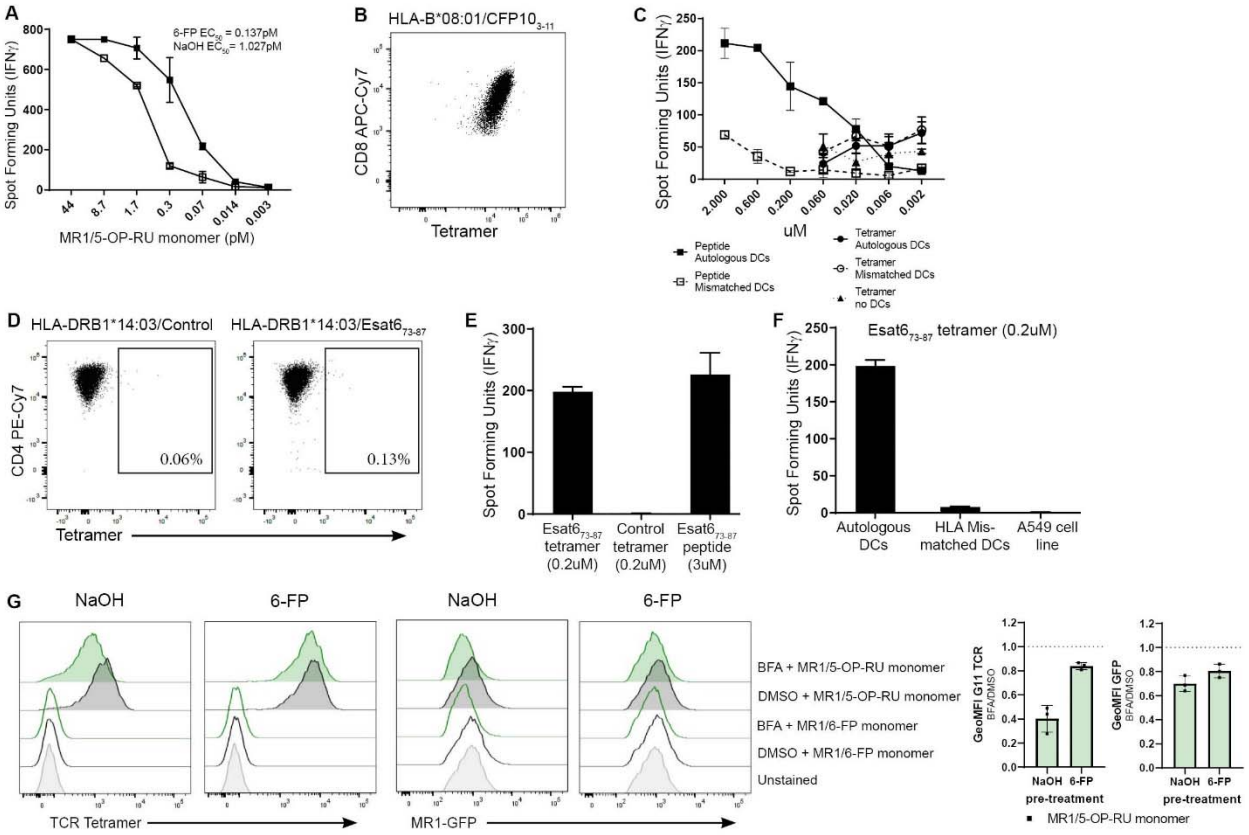

Fig 5. Ligand exchange can occur in post-ER compartments. A. MR1T cell clone (1e4) IFN-γ response to BEAS-2B.MR1-GFP (1e4) that were pretreated with 6-FP *vs* NaOH using MR1/5-OP-RU monomer as the antigen. EC_{50} calculated using non-linear regression and the difference in the EC_{50} was statistically significant between the curves ($p<0.0001$) by the extra sum-of-squares F test. For EC_{50} values of replicate experiments see Supplementary Table 4. **B.** HLA*B08:01-restricted T cell clone D480-F6 was stained with the HLA-B*08:01 tetramer to $CFP10_{3-11}$, along with antibodies to CD3, CD4, CD8 and a live/dead discriminator. Live, $CD3^+CD4^-CD8^+$ T cells are shown. **C.** HLA*B08:01-restricted T cell clone D480-F6 (5e3) IFN-γ response to DCs (1e4) that were incubated with either the $CFP10_{3-11}$ tetramer or $CFP10_{3-11}$ peptide. 9.5e4 irrelevant T cells (MR1-restricted D426-G11) were also added to the well to decrease T:T presentation of the classical T cell clone. **D.** MHC II-restricted T cell clone D481-D1 was stained with the HLA-DRB1*14:03 tetramer to $Esat6_{73-87}$ or a control tetramer along with antibodies to CD3, CD4, CD8 and a live/dead discriminator. Live, $CD3^+CD8^-CD4^+$ T cells are shown. **E.** MHC II-restricted T cell clone D481-D1 (2e4) IFN-γ response to D481 (autologous) dendritic cells (2e4) that were incubated with either the $Esat6_{73-87}$ tetramer, control tetramer or $Esat6_{73-87}$ peptide. **F.** MHC II-restricted D481-D1 T cell clone (2e4) IFN-γ response to D481 (autologous) dendritic cells, D520 mismatched dendritic cells or A549 cells (2e4) that were incubated with the $Esat6_{73-87}$ tetramer. **G.** BEAS-2B.MR1-GFP cells were pre-incubated with 6-FP or NaOH overnight. 6-FP was washed off and cells were incubated with 50 ug/ml brefeldin A (BFA) for 1h before addition of MR1/5-OP-RU or MR1/6-FP monomer for an additional 4 h. Cells were surface stained for flow cytometry with TCR tetramer. Representative histograms are shown on the left with pooled geometric mean

fluorescence intensity from three experiments shown on the right. The same unstained control is shown in all plots. Error bars denote SD. Data in A, C, E and F are representative of three independent experiments. Error bars denote SD between technical duplicates within the representative experiment shown.

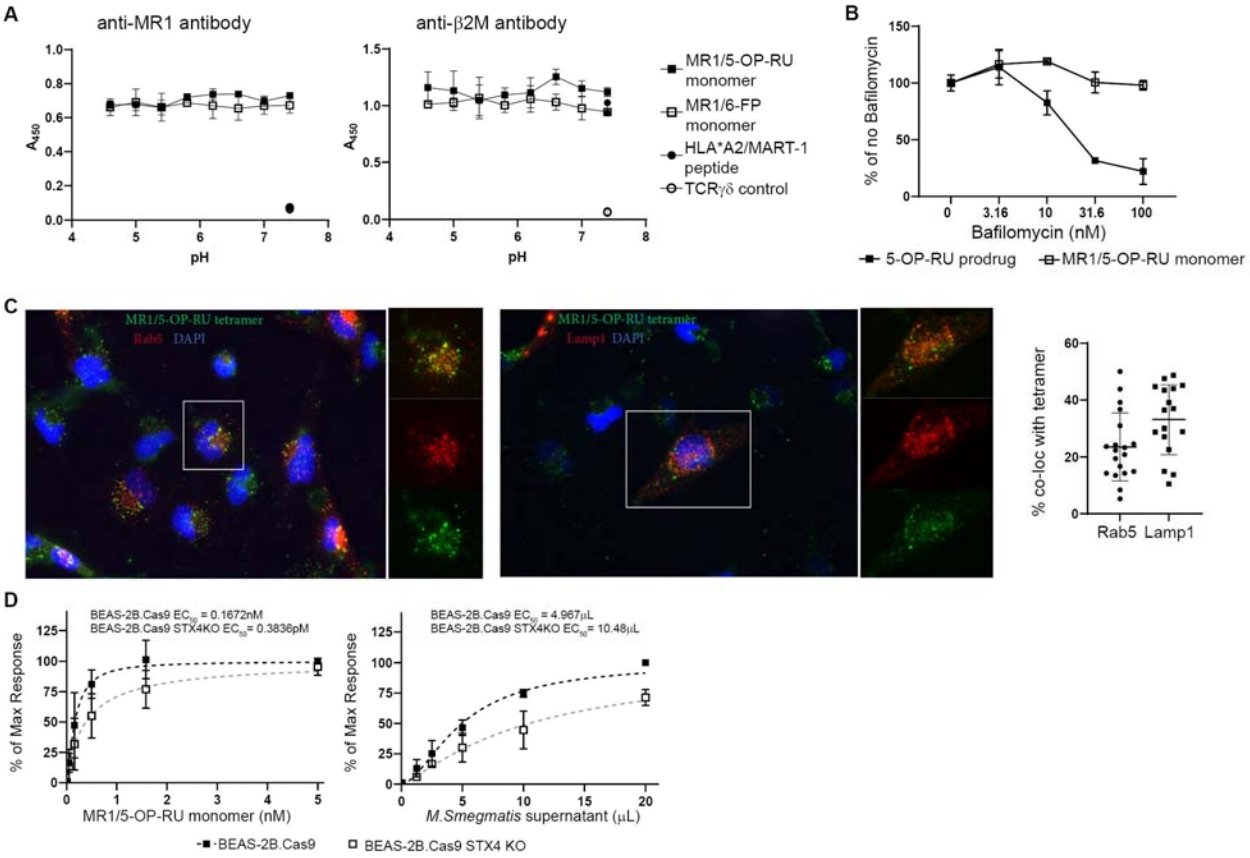

Fig. 6. Ligand exchange does not require acidification.

A. Recombinant, biotinylated MR1 monomer, γδ TCR, or HLA-A2 were immobilized on a traptavidin-coated plate before incubation with PBS at the indicated pH overnight at 4°C. Binding of either anti-MR1 (clone 26.5) or anti-β_2m (clone B2M-01) antibody was assessed with an HRP-conjugated secondary antibody and TMB substrate. A recombinant γδ TCR was included as a negative control and HLA-A2 was included as a positive control for the anti-β_2m antibody and a negative control for the anti-MR1 antibody. Error bars denote SD of 3 replicates. **B.** MR1T cell clone (5e3) IFN-γ response to BEAS-2B (1e4) pre-treated with Bafilomycin A1 for 2 h, followed by addition of the MR1/5-OP-RU monomer or 5-OP-RU prodrug. Data in **B** are representative of three independent experiments. Error bars denote SD between technical duplicates within the representative experiment shown. **C**. BEAS-2B cells (1e5 or 1e4) were seeded on chamber slide and CellLight RFP reagents for Rab5 and LAMP1 were added and incubated for 18 h at 37C. Tetramer was then added for 2 h at RT, followed by washing 2X in PBS. All images acquired were using the same microscope settings. Data are representative of three independent experiments. Error bars denote SD from a representative experiment. **D**. MR1T cell clone (1e3) IFN-γ response to BEAS-2B.Cas9 or BEAS-2B.Cas9 STX4 KO cells (1e4) in the presence of the indicated concentrations of *M. smegmatis* supernatant or MR1/5-OP-RU monomer. Data were normalized to the maximum response and pooled from three experiments. Error bars denote SD. EC_{50} calculated using non-linear regression and the difference in the EC_{50} was statistically significant between the curves (p=0.0032) by the extra sum-of-squares F test.